

Note

Improved synthesis and crystal structure of tetrakis(acetonitrile)(η^4 -1,5-cyclooctadiene)ruthenium(II) bis[tetrafluoroborate(1 –)]

Jason A. Widegren, Heiko Weiner, Susie M. Miller, Richard G. Finke *

Department of Chemistry, Colorado State University, Fort Collins, CO 80523, USA

Received 19 April 2000; received in revised form 6 June 2000

Abstract

An improved, one-step synthesis of $[\text{Ru}^{\text{II}}(1,5\text{-COD})(\text{CH}_3\text{CN})_4]^{2+}$ as the BF_4^- salt has been accomplished in 51% yield, an approximately 75% higher yield than the three-step literature synthesis of the corresponding PF_6^- salt. The improved synthesis consists of (i) grinding the insoluble $[\text{RuCl}_2(1,5\text{-COD})]_x$ precursor to increase the reaction rate and yield, (ii) treating the resultant $[\text{RuCl}_2(1,5\text{-COD})]_x$ with $2\text{Ag}^+\text{BF}_4^-$ in refluxing acetonitrile with excess 1,5-COD present to inhibit 1,5-COD loss in the product and, most importantly, (iii) following the reaction directly by $^1\text{H-NMR}$ spectrometry which revealed that the substitution reaction of the Ru(II), d^6 precursor is, as expected, quite slow and requires ca. 120 h. The $[\text{Ru}(1,5\text{-COD})(\text{CH}_3\text{CN})_4][\text{BF}_4]_2$ product was characterized by ^1H , ^{13}C , and $^{19}\text{F-NMR}$, elemental analysis, and single-crystal X-ray crystallography. Problems in commercial Ru and F analyses are also addressed since this issue has been inadequately treated in the existing literature. © 2000 Elsevier Science S.A. All rights reserved.

Keywords: Acetonitrile solvate of ruthenium; Surface area effects on heterogeneous reaction rates; Improved reaction yields via direct monitoring; X-ray crystal structure; *trans* Influence of olefin and nitrile ligands; Interferences in commercial F and Ru analyses

1. Introduction

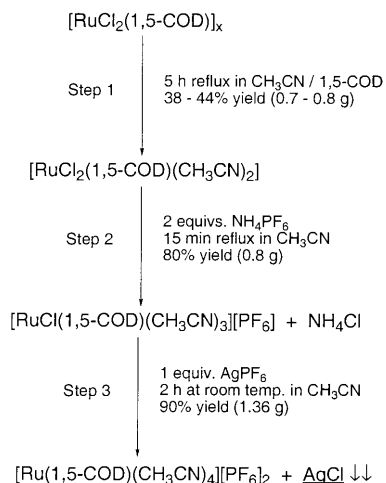
Acetonitrile solvate complexes are widely useful for the synthesis of organometallic compounds because of facile substitution at the solvate coordination sites [1,2]. Similarly, 1,5-cyclooctadiene (1,5-COD) complexes have found considerable use in organometallic chemistry as well [3–5]. Accordingly, we have used the mixed acetonitrile solvate 1,5-COD complexes $[\text{M}^{\text{I}}(1,5\text{-COD})(\text{CH}_3\text{CN})_2][\text{BF}_4]$ ($\text{M} = \text{Ir}, \text{Rh}$) to prepare the polyoxoanion-supported compounds $(\text{Bu}_4\text{N})_5\text{Na}_3[(1,5\text{-COD})\text{M}^{\text{I}}\text{P}_2\text{W}_{15}\text{Nb}_3\text{O}_{62}]$ [6,7]. These polyoxoanion-supported, labile-ligand compounds have then been used to prepare polyoxoanion-stabilized Ir(0) and Rh(0) nanoclusters [8,9], materials which show record catalytic lifetimes in solution from among known nanoclusters [10].

Hoping to extend our studies of polyoxoanion-stabilized nanoclusters to include ruthenium, and with an eye towards ruthenium-based arene hydrogenation, we searched the literature for an appropriate acetonitrile solvate complex of ruthenium from which to synthesize the currently unknown compound $[(1,5\text{-COD})(\text{CH}_3\text{CN})\text{Ru}^{\text{II}}\text{P}_2\text{W}_{15}\text{Nb}_3\text{O}_{62}]^{7-}$. This led us to the literature synthesis of $[\text{Ru}^{\text{II}}(1,5\text{-COD})(\text{CH}_3\text{CN})_4][\text{PF}_6]_2$ [11], Scheme 1.

This literature synthesis requires three steps, beginning from the commercially available starting material $[\text{RuCl}_2(1,5\text{-COD})]_x$, and proceeds with an overall reported yield of 27–32% [11]. A small-scale (ca. 400 mg) preparation of the perchlorate salt, $[\text{Ru}(1,5\text{-COD})(\text{CH}_3\text{CN})_4][\text{ClO}_4]_2$, has also been described [12], but no yield was reported and, of course, the ClO_4^- salt is generally less desirable. Hence, it became important to have a higher yield, preferably one-step synthesis of $[\text{Ru}^{\text{II}}(1,5\text{-COD})(\text{CH}_3\text{CN})_4]^{2+}$.

* Corresponding author. Fax: +1-970-4911801.

E-mail address: rfinke@lamar.colostate.edu (R.G. Finke).



Scheme 1. The three-step, literature synthesis of $[\text{Ru}(1,5\text{-COD})(\text{CH}_3\text{CN})_4][\text{PF}_6]_2$ [11]. The reported, overall yield using this procedure is 27–32% [11].

Herein we describe a straightforward, one-step procedure for preparing $[\text{Ru}(1,5\text{-COD})(\text{CH}_3\text{CN})_4][\text{BF}_4]_2$ (**1**). Our synthesis provides a 51% yield, compared to an overall ca. 30% yield for the three-step literature synthesis of the PF_6^- salt. The resultant $[\text{Ru}(1,5\text{-COD})(\text{CH}_3\text{CN})_4][\text{BF}_4]_2$ has been fully characterized, including by single-crystal X-ray crystallography. In addition, we report the results of F and Ru elemental analyses, experiments performed as controls to test the problems cited in the literature with elemental analyses of these elements.

2. Experimental

2.1. General procedures

All manipulations were performed in air. Elemental analyses were obtained from Galbraith Laboratories, Inc. (Knoxville, TN). Rotary evaporation was accomplished with the aid of a Büchi RE 121 rotary evaporator connected to a Büchi V-500 membrane pump. Nuclear magnetic resonance (NMR) spectra were obtained as CD_2Cl_2 solutions in Spectra Tech or Wilmad NMR tubes (5 mm o.d.) at 25°C on a Varian Inova 300 MHz instrument. Chemical shifts were referenced to SiMe_4 (^1H -NMR and ^{13}C -NMR) or to CFCl_3 (^{19}F -NMR). Spectral parameters for ^1H -NMR (300 MHz) include: tip angle 30° (pulse width 2.9 μs); acquisition time 2.667 s; sweep width 6000 Hz. Spectral parameters for ^{13}C -NMR (75 MHz) include: tip angle 45° (pulse width 4.2 μs); acquisition time 0.8 s; sweep width 20 000 Hz. Spectral parameters for ^{19}F -NMR (282 MHz) include: tip angle 30° (pulse width 4.9 μs); acquisition time 1.252 s; sweep width 50 000 Hz.

2.2. Materials

Acetonitrile (Fisher, certified A.C.S.), ethyl acetate (Aldrich, HPLC grade), ethanol (McCormick Distillery, Inc., anhydrous), 1,5-cyclooctadiene (Aldrich, 99 + %), and silver tetrafluoroborate (Aldrich, 98%) were used as received. Dichloro(1,5-cyclooctadiene)ruthenium(II), $[\text{RuCl}_2(1,5\text{-COD})]_x$ (Strem, 99%), was ground for 15 min with a porcelain mortar and pestle to increase its surface area in the suspended-solid reaction which follows. The $[\text{RuCl}_2(1,5\text{-COD})]_x$ changes from black to brown during the grinding, the lighter color being consistent with a decrease in its particle size.

2.3. Preparation of $[\text{Ru}(1,5\text{-COD})(\text{CH}_3\text{CN})_4][\text{BF}_4]_2$ (**1**)

Recently ground (vide supra) $[\text{RuCl}_2(1,5\text{-COD})]_x$ (4.00 g, 14.3 mmol of Ru) was placed in an oven-dried, 250 ml, round-bottomed, side-armed flask containing a stir bar and 80 ml of acetonitrile. To suppress the loss of 1,5-COD and subsequent formation of $[\text{RuCl}_2(\text{CH}_3\text{CN})_4]$ [11], 6 ml (48.9 mmol) of 1,5-cyclooctadiene was added. Next, AgBF_4 (5.56 g, 28.6 mmol, 2.0 equivalents versus Ru), which had been weighed into a separate glass vial, was added to the stirred suspension. The glass vial was rinsed with 20 ml of acetonitrile and these washings were added to the 250 ml reaction flask. The round-bottomed flask was then fitted with a heating mantle and a reflux condenser, and the reaction mixture was heated under reflux with stirring for 120 h (see Fig. 1, vide infra). The brown suspension gradually lightened in color as the reaction proceeded. The product mixture was allowed to cool to room temperature and was gravity filtered (Whatman # 2 paper) into a 250 ml round-bottomed flask to remove the solid AgCl and unreacted $[\text{RuCl}_2(1,5\text{-COD})]_x$. The filter paper was then rinsed with 50 ml of acetonitrile. The clear, yellow-brown filtrate was reduced in volume to about 20 ml by rotary evaporation at 40°C. Next, 40 ml of ethyl acetate was added dropwise over 15 min with stirring. After about half of the ethyl acetate was added, fine yellow crystals began to form. The solution was stirred for an additional 5 min following the addition. The yellow crystals were then allowed to settle to the bottom of the flask and the supernatant was removed with a polyethylene pipette. The yellow crystals were washed with 2×25 ml of ethyl acetate by adding 25 ml of ethyl acetate to the round-bottomed flask, stirring the mixture for about 2 min, allowing the crystals to settle, and then removing the liquid with a polyethylene pipette. The crystals were then dissolved in a *minimum* amount of acetonitrile (typically ≤ 15 ml) and gravity filtered (Whatman # 2 paper) into a 125 ml Erlenmeyer flask. The filter paper was rinsed with 10 ml of acetonitrile. Anhydrous ethanol was then added until the solution became slightly cloudy (typically 50–100 ml) and the

Erlenmeyer flask was sealed with Parafilm and placed in a -20°C freezer for at least 3 h. The yellow, crystalline product was then collected on a medium glass frit, washed with 3×20 ml of anhydrous ethyl ether, and allowed to dry on the frit under aspiration for 30 min. Yield: 4.01 g (51%). Anal. Found (calc. for $[\text{Ru}(1,5\text{-COD})(\text{CH}_3\text{CN})_4][\text{BF}_4]_2$): C, 35.07 (35.13); H, 4.62 (4.42); N, 10.48 (10.24); B, 3.74% (3.95) [13–17]. $^1\text{H-NMR}$, δ (no. of H, multiplicity): 4.8 (4.0 H, unresolved multiplet), 2.8 (6.1 H, singlet), 2.5 (10.3 H, singlet superimposed on an unresolved multiplet), 2.2 (4.1 H, partially resolved multiplet). $^{13}\text{C-NMR}$, δ : 4.3, 5.2, 29.2, 97.2, 126.1, 130.6. $^{19}\text{F-NMR}$, δ : -152.6 (singlet with a downfield shoulder).

2.4. Procedure for monitoring the evolution of **1** with $^1\text{H-NMR}$

Directly monitoring the reaction's progress proved key to improving the yield and selecting an optimized reaction time. At selected intervals during the reaction, duplicate aliquots of the reaction mixture were removed for analysis by $^1\text{H-NMR}$ (typically, only one of the aliquots was actually analyzed, the second aliquot serving as a backup). Aliquots were removed by opening the side-arm stopcock, inserting a stainless steel needle into the stirred reaction mixture, withdrawing 0.5 ml of solution into a disposable 1 ml syringe, and then closing the sidearm stopcock. The stainless steel needle was then replaced with a nylon-membrane syringe filter (0.2 μm pore size), the aliquot was filtered through the membrane filter, and the filtration process was completed by rinsing the membrane syringe filter with 3×0.5 ml of acetonitrile. The sample was then evacuated to dryness by rotary evaporation at 40°C . Next, the sample was redissolved in 1.5 ml of CD_2Cl_2 (Cambridge Isotope Laboratories, Inc.) and, using a 5 ml glass syringe, filtered through a nylon-membrane syringe filter (0.2 μm pore size) directly into an NMR tube. The relative amount of product was determined by comparing the integral of the ^1H residual of the deuterated dichloromethane solvent peak to the integral of the product peak at δ 4.8 due to the 1,5-cyclooctadiene ligand.

2.5. X-ray crystallography

X-ray quality single crystals were grown from ca. 100 mg of **1** in 25 ml of $\text{CH}_3\text{CN-EtOH}$ (1:9) at -20°C . These conditions are similar to those used to recrystallize the product during a standard preparation of **1**, although about 10 times more dilute. X-ray diffraction data for **1** were collected at 160 K on a Siemens SMART CCD diffractometer. Lorentz and polarization corrections were applied, along with empirical absorption corrections (SADABS [18]). The structure was solved

Table 1
Crystal data and structure refinement for **1**

Empirical formula	$\text{C}_{16}\text{H}_{24}\text{B}_2\text{F}_8\text{N}_4\text{Ru}$
Formula weight	547.08
Wavelength (\AA)	0.71073
Crystal system	Monoclinic
Space group	$P2_1/n$
Unit cell dimensions	
a (\AA)	16.0605(1)
b (\AA)	12.5340(2)
c (\AA)	22.1970(1)
β ($^{\circ}$)	101.207(1)
Volume (\AA^3)	4383.10(8)
Z	8
Absorption coefficient (mm^{-1})	0.793
Crystal size (mm)	$0.16 \times 0.18 \times 0.18$
θ range for data collection ($^{\circ}$)	1.44–28.48
Limiting indices	$-20 \leq h \leq 20$, $-15 \leq k \leq 16$, $-18 \leq l \leq 29$
Reflections collected	28559
Independent reflections	10600 ($R_{\text{int}} = 0.0797$)
Data/restraints/parameters	10598/0/555
Goodness of fit on F^2	0.986
Final R indices ^a	$R_1 = 0.0649$, $wR_2 = 0.1580$
Extinction coefficient	0.00055(12)
Largest difference peak and hole (e \AA^{-3})	2.048 and -1.178

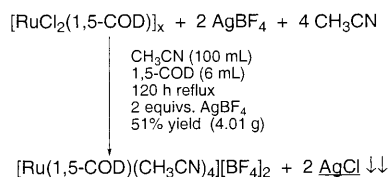
^a R_1 is for $[I > 2\sigma(I)]$, wR_2 is for all data. $R_1 = \Sigma||F_o| - |F_c|| / \Sigma|F_o|$, $wR_2 = [\Sigma w(|F_o| - |F_c|)^2 / \Sigma w|F_o|^2]^{1/2}$.

by direct methods and refined using the Siemens SHELXTL program library [19]. The structure was refined by full-matrix weighted least-squares on F^2 for all reflections. All non-hydrogen atoms were refined with anisotropic displacement parameters. Hydrogen atoms were included in the structure factor calculations at idealized positions. Selected crystal data and structural refinement parameters are collected in Table 1.

3. Results and discussion

3.1. Preparation of $[\text{Ru}(1,5\text{-COD})(\text{CH}_3\text{CN})_4][\text{BF}_4]_2$

The synthesis of $[\text{Ru}(1,5\text{-COD})(\text{CH}_3\text{CN})_4][\text{BF}_4]_2$ (**1**) was accomplished in 51% yield in one step using two equivalents of AgBF_4 to remove the chloride from the



Scheme 2. The one-step, 51% yield synthesis of $[\text{Ru}(1,5\text{-COD})(\text{CH}_3\text{CN})_4][\text{BF}_4]_2$ (**1**) developed herein. Note that reflux is 78°C at the mile-high altitude of our laboratories at Colorado State University.

$[\text{RuCl}_2(1,5\text{-COD})]_x$ starting material (Scheme 2). The simple, but crucial, key to improving the yield of **1** involved following the reaction's progress directly by $^1\text{H-NMR}$ (Fig. 1).

Fig. 1 shows two important points: the substitution reaction on the d^6 , Ru(II) precursor is slow as expected even in refluxing CH_3CN , and the formation of product has slowed to a near-zero rate after about 100 h at 78°C reflux. Interestingly, and as shown in Fig. 1, the data (including the fact that the reaction yield maximizes around 50%) are reasonably well fit by the integrated rate equation for an $\text{A} \rightarrow \text{B} \rightarrow \text{C}$ reaction sequence (see Eqs. 4–6 elsewhere, [20]), where A is $[\text{RuCl}_2(1,5\text{-COD})]_x$, B is **1**, and C is presently unidentified. The data could not be fit using a single exponential function, specifically the integrated rate equation corresponding to the other most obvious possible mechanism to two products, the parallel reactions $\text{A} \rightarrow \text{B}$ (rate constant k_1) and $\text{A} \rightarrow \text{C}$ (rate constant k_2)¹.

We reasoned that the reaction rate and yield could be further improved by increasing the surface area of the insoluble $[\text{RuCl}_2(1,5\text{-COD})]_x$, since such heterogeneous, liquid–solid reactions typically show a dependence on the surface area of the insoluble material² [21,22]. Indeed, grinding the $[\text{RuCl}_2(1,5\text{-COD})]_x$ starting mate-

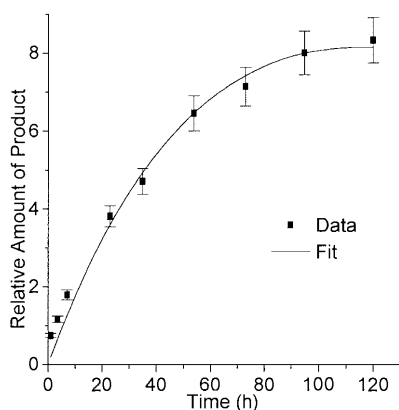


Fig. 1. Plot of the reaction progress versus time for the synthesis of **1**. The evolution of product was monitored by removing aliquots of the reaction solution and then analyzing them by $^1\text{H-NMR}$. Note that the final data point (at 120 h), for which the relative amount of product equals 8.3, corresponds to an *isolated* yield of 51%. The solid line shows the fit of the kinetic data to the integrated rate equation given in Eqs. 4–6 elsewhere [20] corresponding to an $\text{A} \rightarrow \text{B} \rightarrow \text{C}$ reaction sequence (where A is the $[\text{RuCl}_2(1,5\text{-COD})]_x$, B is **1**, and C is an unidentified, follow-up product) and using Microcal's Origin software (version 3.5.4).

¹ The integrated rate equation for [B] formation for the parallel pathways mechanism, derivable via a couple of pages of algebra, is $[\text{B}]_\infty / ([\text{B}]_\infty - [\text{B}]_t) = e^{-k_{\text{obs}}t}$, where $k_{\text{obs}} = k_1 + k_2$.

² See ref. [21] for a theoretical study of the effect of particle size and particle size distribution on reaction kinetics in liquid–solid heterogeneous reactions. See ref. [22] for a study of the effect of surface area on the heterogeneous reaction of quartz powder with aqueous sodium hydroxide.

rial in a mortar and pestle prior to the reaction increased the isolated yield from 42% to 51% for a 120 h reaction.

The following evidence establishes the purity of the resultant **1**. First, the C, H, N and boron analyses each match the calculated values for pure compound. Second, the combination of the boron analysis and a $^{19}\text{F-NMR}$ spectrum showing no visible ($< 5\%$) impurities in the -300 ppm to $+300$ ppm range demonstrates the purity of the anionic, BF_4^- component of **1** (this is not trivial, as this and related anions are known to decompose [23]). Third, **1** is 97% pure by $^1\text{H-NMR}$, which confirms the (reliable) C, H and N analyses and, hence, the purity of the organic components of **1**. In short, given that the C, H, N and boron elements in **1** have been shown to be present in the correct proportion, it follows that the F (present only as BF_4^- by $^{19}\text{F-NMR}$) and, then, Ru must also be present in the correct proportions; in short, there is no other way to fit the C, H, N and B (and thus F and thus, by difference, Ru) analyses³.

³ The reader may wonder, as we did, why F and Ru analyses are commonly *not* performed on organoruthenium complexes. (They were not reported in ref. [11] for example.) In addition to their expense, a simple answer is that reliable analyses can be difficult to obtain for these particular elements and depending upon what interfering elements are present. Let us first consider the case of F analysis, which is commonly determined, after sample combustion, by F^- selective electrode (for example, this is the standard method used by Galbraith Laboratories Inc., *vide infra*). However, it is well known that interference by B can give spurious results [13,14] when using F^- selective electrode. In fact, at least one literature report [13] demonstrates that this technique gives a 9% low F analysis of a BF_4^- salt [Anal. Found (calc. for $[\text{C}_7\text{H}_{14}\text{NOS}][\text{BF}_4]$): F, 21.5 (30.76)]. The reader might also wonder, as we did, what would result if we did the control experiment and obtained F and Ru analyses on **1**, a compound proven to be pure by a variety of other methods, but also a BF_4^- salt and, of course, a complex of Ru. In fact, a F analysis on **1** (as performed by Galbraith Laboratories Inc.) *proved unreliable as expected* (low by almost 4%) [Anal. Found (calc. for $[\text{Ru}(1,5\text{-COD})(\text{CH}_3\text{CN})_4][\text{BF}_4]_2$): F, 23.92 (27.28)]. Note that the true error bars on this analysis must be $\pm 4\%$.

The case for Ru analysis based on the existing literature is a little less clear, but still instructive.

Arguably the best method of Ru analysis is inductively coupled plasma atomic emission spectrometry (ICP-AES) [15]. However, even ICP-AES is known to suffer from a variety of interferences that generally become more difficult to overcome the more complicated the sample [15–17]. Again we did the control experiment of obtaining a Ru analysis by ICP-AES and via Galbraith Laboratories (i.e. where all the other analyses had been obtained). Indeed, and in two independent analyses, the Ru analysis came out about 3% lower than the calculated value (calc. 18.47, found 15.35, 15.77). Hence there does appear to be an unidentified interference or other problem in at least this specific analysis, one that reduces the reliability of this specific Ru analysis to $\pm 3\%$. The take-home message seems clear: one must be careful when interpreting results of at least some commercial F and Ru analyses on difficult samples since the standard methods and procedures are not foolproof and *since realistic error bars are not provided as a part of the analysis. Caveat emptor!*

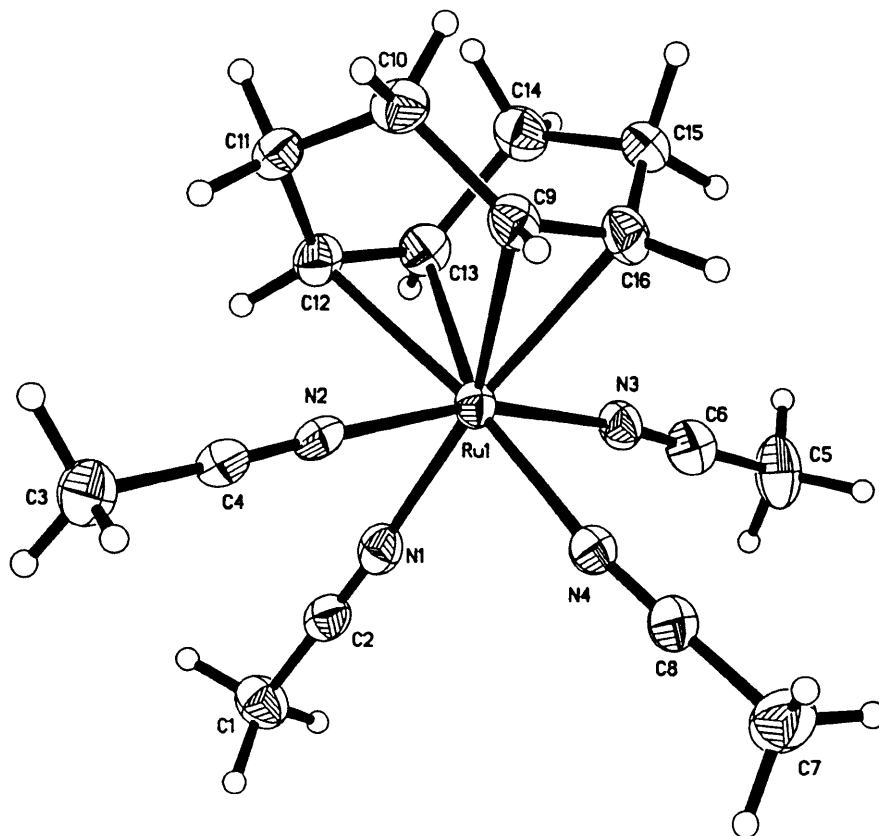


Fig. 2. Molecular structure and atomic numbering scheme for **1** with thermal ellipsoids shown at the 50% probability level.

3.2. Comparison of the preparation of $[Ru(1,5-COD)(CH_3CN)_4][BF_4]_2$ to the preparation of $[Ru^{II}(1,5-COD)(CH_3CN)_4][PF_6]_2$

The literature preparation of $[Ru^{II}(1,5-COD)(CH_3CN)_4][PF_6]_2$ described in Section 1 (Scheme 1) and the preparation of **1** (Scheme 2) involve similar chemistry. An advantage of the literature synthesis would appear to be the overall time required to go from $[RuCl_2(1,5-COD)]_x$ to $[Ru^{II}(1,5-COD)(CH_3CN)_4][PF_6]_2$ (about 3 days) which is shorter than the time required by the present synthesis to go from $[RuCl_2(1,5-COD)]_x$ to **1** (about 5 days). However, the synthesis of $[Ru^{II}(1,5-COD)(CH_3CN)_4][PF_6]_2$ is done in a stepwise manner [11], which is considerably more work than the present preparation of **1**, especially since the second step of the literature synthesis must be done *twice* to have enough material to perform the third step of the literature synthesis. The literature synthesis of $[Ru^{II}(1,5-COD)(CH_3CN)_4][PF_6]_2$ [11] also results in only a 27–32% overall yield in comparison to the 51% yield of **1** herein, a yield that Fig. 1 shows is optimized at least as far as the reaction time is concerned (and for grinding of the starting material to improve its surface area and, thereby, the resultant reaction rate). This ca. 75% increase in percent yield is made even more significant by

the expense of the $[RuCl_2(1,5-COD)]_x$ precursor, presently about \$60 per gram.

3.3. Crystal structure of $[Ru(1,5-COD)(CH_3CN)_4][BF_4]_2$

The molecular structure (with thermal ellipsoids shown at the 50% probability level) and atomic numbering scheme for **1** are shown in Fig. 2. Selected bond lengths and bond angles are shown in Table 2. There are actually two molecules of **1** in the asymmetric unit, but the bond lengths and bond angles are similar for both molecules. For example, the Ru–C bond distances in molecule 1 (shown in Fig. 2) are 2.255(6), 2.243(6), 2.241(6) and 2.230(6) Å compared to 2.240(5), 2.238(6), 2.238(6) and 2.226(6) Å for molecule 2.

Table 2
Selected bond lengths (Å) and bond angles (°) for **1**

Ru1–N1	2.061(5)	Ru1–N2	2.037(5)
Ru1–N3	2.036(5)	Ru1–N4	2.069(5)
Ru1–C9	2.255(6)	Ru1–C12	2.230(6)
Ru1–C13	2.241(6)	Ru1–C16	2.243(6)
N1–Ru1–N2	85.6(2)	N1–Ru1–N3	84.3(2)
N1–Ru1–N4	93.6(2)	N2–Ru1–N3	165.6(2)
N2–Ru1–N4	85.6(2)	N3–Ru1–N4	84.8(2)

The six-coordinate ruthenium atom exhibits distorted octahedral geometry. The two acetonitrile ligands *trans* to one another are bent away from the 1,5-COD ligand (the N2–Ru1–N3 bond angle is 165.6(2)°, and the corresponding N–Ru–N angle in the other molecule of **1** in the asymmetric unit is 163.1(2)°). The two acetonitrile ligands *trans* to the 1,5-COD ligand have longer Ru–N bond lengths (2.061(5) and 2.069(5) Å, and for the other molecule of **1** in the asymmetric unit, 2.052(5) and 2.053(5) Å) compared to the two acetonitrile ligands which are *trans* to one another (2.037(5) and 2.036(5) Å, and for the other molecule of **1** in the asymmetric unit, 2.023(5) and 2.027(5) Å). The ca. 0.03 Å difference in length for the Ru–N bonds *trans* to olefin compared to the Ru–N bonds *trans* to nitrile is apparently due to the *trans* influence [24]. Both olefin and nitrile ligands have a relatively low *trans* influence [24,25], but in this complex the *trans* influence of the olefin is found to be higher. The crystal structures of other ruthenium complexes with both acetonitrile and 1,5-COD ligands have been reported [26–29], but the structure of **1** is the first with acetonitrile ligands *trans* to the 1,5-COD ligand and in a ruthenium complex.

4. Conclusions

The ruthenium solvate complex $[\text{Ru}^{\text{II}}(1,5\text{-COD})(\text{CH}_3\text{CN})_4]^{2+}$ has been prepared as its BF_4^- salt in a single step and in 51% yield, an approximately 75% increase in yield over the literature, three-step synthesis of the analogous PF_6^- complex. An X-ray crystal structure of the complex was determined, the first structure of $[\text{Ru}^{\text{II}}(1,5\text{-COD})(\text{CH}_3\text{CN})_4]^{2+}$. Given the usefulness of labile-ligand acetonitrile and 1,5-COD complexes [1–5], the present complex promises to find applications not only in our own work, but also the work of others.

5. Supplementary material

Crystallographic data for the structural analysis have been deposited with the Cambridge Crystallographic Data Centre, CCDC no. 137679 for compound **1**. Copies of this information may be obtained free of charge from The Director, CCDC, 12 Union Road, Cambridge CB2 1EZ, UK (Fax: +44-1223-336033; e-mail: deposit@ccdc.cam.ac.uk or www: http://www.ccdc.cam.ac.uk).

Acknowledgements

We thank Professor Oren P. Anderson (Colorado State University) for reading the manuscript from his perspective as an expert crystallographer, and Professor Steve Strauss for his thoughts on the problems with F and Ru analyses. We thank the Department of Energy, Chemical Sciences Division, Office of Basic Energy for providing financial support for this research via grant DOE FG06-089ER13998.

References

- [1] J.P. Collman, L.S. Hegedus, J.R. Norton, R.G. Finke, Principles and Applications of Organotransition Metal Chemistry, University Science Books, Mill Valley, CA, 1987, p. 199.
- [2] K.R. Dunbar, Comments Inorg. Chem. 13 (1992) 313.
- [3] R.R. Schrock, J.A. Osborn, J. Am. Chem. Soc. 93 (1971) 3089.
- [4] P.W. Jolly, G. Wilke, The Organic Chemistry of Nickel, vols. 1 and 2, Academic Press, New York, 1974 and 1975.
- [5] F.G.A. Stone, Acc. Chem. Res. 14 (1981) 318.
- [6] K. Nomiya, M. Pohl, N. Mizuno, D.K. Lyon, R.G. Finke, Inorg. Synth. 31 (1997) 186.
- [7] M. Pohl, D.K. Lyon, N. Mizuno, K. Nomiya, R.G. Finke, Inorg. Chem. 34 (1995) 1413.
- [8] J.D. Aiken III, Y. Lin, R.G. Finke, J. Mol. Catal. A: Chem. 114 (1996) 29.
- [9] J.D. Aiken III, R.G. Finke, J. Mol. Catal. A: Chem. 145 (1999) 1.
- [10] J.D. Aiken III, R.G. Finke, J. Am. Chem. Soc. 121 (1999) 8803.
- [11] M.O. Albers, T.V. Ashworth, H.E. Oosthuizen, E. Singleton, Inorg. Synth. 26 (1989) 68.
- [12] R.R. Schrock, B.F.G. Johnson, J. Lewis, J. Chem. Soc. Dalton Trans. (1974) 951.
- [13] M.B. Terry, F. Kasler, Mikrochim. Acta (1971) 569.
- [14] H.-C. Wang, Fen Hsi Hua Hsueh 8 (1980) 553.
- [15] G.L. Moore, Introduction to Inductively Coupled Plasma Atomic Emission Spectrometry, Elsevier, Amsterdam, 1989.
- [16] S. Calmotti, C. Dossi, S. Recchia, G.M. Zanderighi, Spectrosc. Eur. 8 (1996) 18.
- [17] M.M.M. El-Defrawy, J. Posta, M.T. Beck, Anal. Chim. Acta 102 (1978) 185.
- [18] G.M. Sheldrick, SADABS: A Program for Siemens Area Detection Absorption Correction, to be published.
- [19] G.M. Sheldrick, SHELXTL, Siemens, Madison, WI, 1996, Version 5.
- [20] J.H. Espenson, Chemical Kinetics and Reaction Mechanisms, McGraw-Hill, New York, 1981, Chapter 4.
- [21] B. Lakatos, T. Blickle, Acta Chim. Hung. 127 (1990) 395.
- [22] A. Packter, Z. Phys. Chem. Leipzig 260 (1979) 561.
- [23] S.H. Strauss, Chem. Rev. 93 (1993) 927.
- [24] T.G. Appleton, H.C. Clark, L.E. Manzer, Coord. Chem. Rev. 10 (1973) 335.
- [25] D. Fraccarollo, R. Bertani, M. Mozzon, U. Belluco, R.A. Michelin, Inorg. Chim. Acta 201 (1992) 15.
- [26] T.V. Ashworth, D.C. Liles, D.J. Robinson, E. Singleton, N.J. Coville, E. Darling, A.J. Markwell, S. Afr. J. Chem. 40 (1987) 183.
- [27] D. Attanasio, F. Bachechi, L. Suber, J. Chem. Soc. Dalton Trans. (1993) 2373.
- [28] M.A. Bennett, A.C. Willis, L.Y. Goh, W. Chen, Polyhedron 15 (1996) 3559.
- [29] H.E. Selnau Jr., J. Mahmoud, L.C. Porter, Inorg. Chim. Acta 224 (1994) 125.